

G. Telesca, I. Ivanova-Stanik, R. Zagorski, S. Brezinsek,
A. Czarnecka, P. Drewelow, C. Giroud, S. Marsen,
M. Wischmeier and JET EFDA contributors

Numerical Simulations of JET Discharges with the ITER-Like Wall for Different Nitrogen Seeding Scenarios

“This document is intended for publication in the open literature. It is made available on the understanding that it may not be further circulated and extracts or references may not be published prior to publication of the original when applicable, or without the consent of the Publications Officer, EFDA, Culham Science Centre, Abingdon, Oxon, OX14 3DB, UK.”

“Enquiries about Copyright and reproduction should be addressed to the Publications Officer, EFDA, Culham Science Centre, Abingdon, Oxon, OX14 3DB, UK.”

The contents of this preprint and all other JET EFDA Preprints and Conference Papers are available to view online free at www.iop.org/Jet. This site has full search facilities and e-mail alert options. The diagrams contained within the PDFs on this site are hyperlinked from the year 1996 onwards.

Numerical Simulations of JET Discharges with the ITER-Like Wall for Different Nitrogen Seeding Scenarios

G. Telesca¹, I. Ivanova-Stanik², R. Zagorski², S. Brezinsek³,
A. Czarnecka², P. Drewelow⁴, C. Giroud⁵, S. Marsen⁴,
M. Wischmeier⁶ and JET EFDA contributors*

JET-EFDA, Culham Science Centre, OX14 3DB, Abingdon, UK

¹*Department of Applied Physics, Ghent University, B-9000 Gent, Belgium*

²*Institute of Plasma Physics and Laser Microfusion, EURATOM/IPPLM Association, Warsaw, Poland*

³*IEK-4, FZ Jülich GmbH, Association EURATOM-FZJ, TEC, Jülich, Germany*

⁴*Max-Planck-Institut fuer Plasmaphysic, EURATOM Association, D-17491 Greifswald Germany.*

⁵*EURATOM/CCFE Fusion Association, Culham, Abingdon, Oxon. OX14 3DB, UK*

⁶*Max-Planck-Institut fuer Plasmaphysic, EURATOM Association, D-8578 Garching, Germany.*

** See annex of F. Romanelli et al, "Overview of JET Results",
(24th IAEA Fusion Energy Conference, San Diego, USA (2012)).*

ABSTRACT

Two classes of nitrogen seeded pulses are here considered: pulses at high triangularity, high confinement with moderate gas puffing and N seeding rates and pulses at low triangularity, lower confinement with higher gas puffing and N seeding. For the high-delta pulses the power radiation fraction, f_{rad} , is normally about 0.5 while at low delta f_{rad} as high as 0.7 is achieved. For the simulations we have used COREDIV code, which self-consistently couples the plasma core with the plasma edge and the main plasma with impurities. To reproduce numerically the main experimental parameters both for the core and for the SOL plasmas different settings had to be applied to COREDIV, as the perpendicular transport and recycling in the SOL and the power deposition profile in the core. Simulations suggest that higher values for f_{rad} might be achieved with N seeding only at low density and/or higher heating power.

1. INTRODUCTION

A major effort is presently being devoted at JET with the new ITER-like wall (ILW, Be wall and W divertor) to implementing scenarios with impurity seeding. Indeed, in view of developing reactor relevant scenarios, the naturally occurring power radiated fraction (f_{rad}) with the ILW, induced solely by D and Be [1], is too low (< 30%) to protect effectively the target plates from high power loads. However, it is not sufficient to simply increase the power radiated level by seeding impurities, but also the spatial distribution of the power radiated matters. Indeed, the total radiation pattern must be such that the power is not radiated mainly in the very centre of the plasma (for obvious confinement implications), but also some care should be taken with the level of the radiating mantel in the plasma edge, in order to avoid H-L mode back transition. N, Ne and Ar seeding are presently being tested at JET for different magnetic configurations and scenarios. Most experiments have been performed with N seeding so far, while only relatively few with Ne and Ar seeding. In this contribution we limit ourselves to the main aspects of nitrogen seeding experiments and to develop a consistent numerical modelling approach. The general idea with N seeding is to cool down the divertor plasma by increasing radiation in the SOL and around the X-point (maximum of N radiation function around 30eV). In parallel the radiation cooling leads to low impact energies for the intrinsic impurities as well as for N itself, which generally ends up with the control of the W flux, and by consequence of the W radiation level in the main plasma. With respect to nitrogen seeding, two main lines of experiments, at $I_p = 2.5\text{MA}$ and $B_t = 2.7\text{T}$, are being pursued at JET and are modelled in this study: experiments at high triangularity (up = 0.4, low = 0.34) [2] with $H_{98(y,2)}$ up to 0.85 and moderate f_{rad} (< 0.55) and experiments at low triangularity (up = 0.2, low = 0.25) [3] with $H_{98(y,2)}$ up to 0.72 and f_{rad} as high as 0.75. The input power for all the pulses here considered is in the range 18-20MW, mostly supplied by NBI, but also by ICRF central heating. For the simulations we have used COREDIV code [4], which self-consistently couples the plasma core with the plasma edge and the main plasma with impurities. In particular, the code has been validated against nitrogen and neon seeded ELMy H-mode JET discharges with carbon wall [5]

as well as L-mode JET ILW discharges [6], proving its capability of reproducing the main features of JET discharges. Production as well as flushing out of W due to ELMs is not accounted for in the model. Indeed, a steady state W sputtering source is “simulated” in the steady state version of COREDIV, which is presently being used (please, see Sect.2)

In Sect. 2, a brief description of the code is presented. Sect. 3 deals with the discussion of the experimental data as well as with numerical modelling of few typical N seeded discharges and in Sect. 4 the conclusions are drawn.

2. THE COREDIV CODE

Since the energy balance depends strongly on the coupling between the bulk and the scrape-off layer (SOL) plasma, modeling requires the transport problem to be addressed in both regions simultaneously. The physics model used in the COREDIV code is based on a self-consistent coupling of the radial transport in the core to the 2D multi-fluid description of the SOL. Since the model is relatively complex [4, 7] we point out only the aspects relevant to the present study.

2.1 IN THE CORE

The 1D radial transport equations for bulk ions, for each ionization state of impurity ions and for the electron and ion temperature are solved. The electron and ion energy fluxes are defined by the local transport model proposed in ref. [8] which reproduces a prescribed energy confinement law. In particular, the anomalous heat conductivity is given by the expression $\chi_{e,i} = C_{e,i} \frac{a^2}{\tau_E} F(r)$ where r is the radial coordinate, a is the plasma radius, τ_E is the energy confinement time defined by the ELMy H-mode scaling law and the coefficient ($C_e = C_i$) is adjusted to have agreement between calculated and experimental confinement times. The parabolic-like profile function $F(r)$ can be modified at the plasma edge to provide for a transport barrier of chosen level. The main plasma ion density is given by the solution of the radial diffusion equation with diffusion coefficients $D_i = D_e = 0.1\chi_e$. For the auxiliary heating, parabolic-like deposition profile is assumed to be $P_{AUX}(r) = P_0 (1-r^2/a^2)^y$ where y is in the range 1.5–3.

In consideration of the relatively low confinement ($H_{98(y,2)} < 0.72$) of the low-delta discharges heated by NBI only, and of the significant fraction of ICRF heating used for the sawtooth discharges at high-delta, neither of them showing any tendency to impurity accumulation, the numerical radial impurity transport is described only by anomalous diffusion, without pinch.

2.2 IN THE SOL

We use the 2D boundary layer code EPIT, which is primarily based on Braginskii-like equations for the background plasma and on rate equations for each ionization state of each impurity species [9]. An analytical description of the neutrals is used, based on a simple diffusive model. COREDIV takes into account the plasma (D, Be and seeded impurities) recycling in the divertor as well as the sputtering processes at the target plates including deuterium sputtering, self-sputtering and sputtering

due to seeded impurities. (For deuterium sputtering and tungsten self-sputtering the yields in ref. [10] are used). The recycling coefficient is an external parameter which in COREDIV depends on the level of the electron density at the separatrix, n_{e_sep} , given as an input. A simple slab geometry (poloidal and radial directions) with classical parallel transport and anomalous radial transport ($D_{SOL} = \chi_i = 0.5 \chi_e$, where χ_e ranges typically 0.5–1m²/s), is used and the impurity fluxes and radiation losses by impurity ions are calculated fully self-consistently. All the equations are solved only from the midplane to the divertor plate, assuming inner-outer symmetry of the problem.

Comparison of the results of steady state COREDIV simulations with ELMy–H mode experimental data for the W fluxes and concentrations, averaged over times of the order of the particle confinement time, shows that an increase (up to 50–60%) of the W sputtering yield is generally sufficient for realistic COREDIV simulations of ELMy pulses (see, for example ref.[11]).

3. EXPERIMENTS AND MODELLING

3.1

Both the experiments at high and low triangularity were performed in vertical target configuration, to enhance the divertor closure and neutral compression, and for both of them the N seeding was accompanied by substantial gas puffing, mainly in the PFR. For the experiments at high-delta the D puffing rate is in the range 2–3 x 10²² el/s and for the low-delta ones 3 – 5 x 10²² el/s with few cases up to 1 x 10²³ el/s. Nitrogen seeding for high-delta is in the range 2–4 x 10²² el/s while for low-delta it is, in average, a factor of 2 higher with few cases up to 2 x 10²³ el/s. In general, the difference in puffing and seeding levels implies that in high-delta configuration the discharge is mainly attached with temperature at the strike points (T_{e_pl}) of the order of 5–7 eV and significant fraction of the total power radiated in the plasma core, while in low-delta the discharge is semi/fully (depending on the gas puff rate) detached with $T_{e_pl} < 3\text{--}4\text{eV}$ and, on average, power radiated substantially in the SOL and around the X-point (threshold for W sputtering by N at about 4eV). Related with higher triangularity and lower D puffing rate, the high-delta discharges show higher confinement than those low-delta ($H_{98} = 0.80\text{--}0.85$ and $H_{98} = 0.65\text{--}0.72$, respectively), resulting in a flatter density and more peaked temperature profiles, compared with those for the low-delta ones, see Figure 1.

High confinement and low ELM frequency (f_{ELM} order of 20–30Hz) imply that high-delta pulses at the lowest puffing rates are prone to impurity (W) accumulation and radiation collapse if at least 3–4MW (15–20% of input power) are not provided by ICRF central heating with related sawtooth activity [12]. In this study, we have considered only the steady state ICRF heated discharges. For these pulses the power deposition profile prescribed in COREDIV is more peaked than that for the low-delta ones (powered only by NBI), according to the expression $P_{AUX} = P_0(1 - r^2/a^2)^y$, with $y = 1.5$ for NBI heating and 2.5 for high-delta with ICRF central heating (see Sect.2).

In Sect 3.2, we discuss the simulation of two discharges, pertaining to the two scenarios, with similar total input power level ($\sim 20\text{MW}$), similar volume average electron density ($\langle n_e \rangle \sim 7.2x$

10^{19} m^{-3}), similar total radiated power ($\sim 10.6 \text{ MW}$), but different in puffing and seeding level. In 3.3 the simulation of a pulse low-delta at higher radiated power fraction is discussed.

3.2

The tomographic reconstruction of bolometric signals, Figure 2, shows that the power radiated density around the X-point and in the divertor region is somewhat higher for low-delta (JPN 85428, $t = 14 \text{ s}$) than for the high-delta (JPN 85270, $t = 15 \text{ s}$) pulse. Symmetrically, the power radiated in the core is higher for the high-delta pulse, as can be seen from the extended radiation pattern in the low field side.

The COREDIV results for the total power radiated in the SOL and in the confined plasma are 6.8 MW and 3.8 MW for the low-delta and 3.3 MW and 7.1 MW for the high-delta, respectively, similar to the experimental values, within the error bars. In COREDIV it has been set (please, see Sect.2) $n_{e_sep} = 3.9 \times 10^{19} \text{ m}^{-3}$ and $D_{SOL} = 0.35 \text{ m}^2/\text{s}$ for the low-delta, and $3.5 \times 10^{19} \text{ m}^{-3}$ and $0.25 \text{ m}^2/\text{s}$, respectively, for the high-delta. In fact, differences in puffing and seeding levels generally imply differences in recycling fluxed (and in the related density at the separatrix, n_{e_sep}) and in the perpendicular diffusion coefficient in the SOL. For the low-delta pulse, combination of higher seeding rate, higher n_{e_sep} and higher D_{SOL} leads to higher radiation level in the SOL, higher divertor density, lower T_{e_pl} and, consequently, lower W sources and influxes as well as lower power radiated in the core. The calculated central plasma W concentrations, $c_W = 1.9 \times 10^{-5}$ for the low-delta pulse and 4.2×10^{-5} for the high-delta, have to be compared to the experimental ones [13]: 3×10^{-5} and 5×10^{-5} , respectively. Although c_W is higher for the high-delta pulse, the effective ion charge (dominated by nitrogen concentration) is higher for the low-delta pulse, as can be seen from the numerical Z_{eff} in Figure 3, which reproduces fairly well the experimental values. With respect to the COREDIV recycling fluxes, $\Gamma_D = 8.85 \times 10^{23}/\text{s}$ for low-delta and $5.7 \times 10^{23}/\text{s}$ for high-delta, only that for the high-delta can be compared to the experimental one, $\Gamma_D = 4.4 \times 10^{23}/\text{s}$. Indeed, mainly due to the simplified SOL geometry as well as the neutrals model in COREDIV (see Sect.2), it is difficult to compare simulation-experiment in the case of significant recombination. Also due to recombination in the low-delta pulse, only the COREDIV strike point temperature for the high-delta, $T_{e_pl} = 5.1 \text{ eV}$ can be compared with the experimental one, for the outer leg, $T_{e_pl} = 5.5 \text{ eV}$.

3.3

A low-delta pulse at high radiative fraction $f_{rad} \sim 0.7$, $P_{in} = 18 \text{ MW}$, $P_{rad} \sim 13 \text{ MW}$, (JPN 85067, $t = 11.5$), experimentally reached by increasing the N seeding up to $1.4 \times 10^{23} \text{ el/s}$ while keeping the gas puffing rate at a moderate level, has been modelled resulting in the following values for the total power radiated: $P_{rad}(SOL) = 5.4 \text{ MW}$ and $P_{rad}(core) = 7.3 \text{ MW}$. In COREDIV, the core radiation is dominated by W with minor contribution from N, and in the SOL nitrogen radiation accounts for about 3.0 MW with CX losses in excess of 1 MW. Although the COREDIV total level of core radiation is similar to the experimental one, this numerical result is not fully comparable

with the bolometric data, which, within the error bars, seem to indicate a peak of N radiation inside the separatrix, just above the X-point. Indeed, as a consequence of the 1D model for the core (see Sect.2), COREDIV cannot compute poloidal gradients in the core. Due to the large amount of N seeding, the numerical Z_{eff} is as high as 1.6, to be compared to the experimental one $Z_{eff} = 1.7$. Note, however, that this value is only marginally higher (~ 0.5) than that for the ILW baseline, and it is lower than that for unseeded plasmas with carbon surrounding. Further increase of N seeding rate does not lead in COREDIV to increase in P_{rad} , due to extremely low temperatures in the divertor (see ref. [14]). Indeed, for these conditions, the marginal increase in SOL radiation is balanced by further decrease in the W influxes and in the core radiation. Only by decreasing the electron density and/or by increasing the heating power, higher values for f_{rad} might be numerically reached with N seeding, see also ref. [11].

SUMMARY AND CONCLUSION.

For the two examined JET pulses, the high delta-high confinement and the low delta- lower confinement, the power radiated fraction is similar ($f_{rad} \sim 0.52$), but the experimental as well the simulated radiation patterns are different: more radiation in the core for high-delta and more in the SOL for low- delta. This is mainly caused by the different levels of puffing and N seeding rate in the two pulses, which result in different setting in COREDIV: higher density at the separatrix and higher perpendicular transport in the SOL for the low-delta case.

Differently from carbon plate with N seeding [5], for the ILW it seems to be difficult, both experimentally and numerically, to increase f_{rad} above 0.7–0.75 with only N seeding for high density pulses and for heating power around 20MW. At lower density/higher heating power the conditions for higher radiative fraction might be fulfilled.

ACKNOWLEDGEMENTS

This work was supported by EURATOM and carried out within the framework of the European Fusion Development Agreement. The views and opinions expressed herein do not necessarily reflect those of the European Commission.

REFERENCES

- [1]. S. Brezinsek, et al., Journal of Nuclear Materials **438** (2013) 303
- [2]. C. Giroud, et al., Nuclear Fusion **53** (2013) 113025
- [3]. M. Wischmeier, this Conference
- [4]. R. Zagorski, et al., Contributions to Plasma Physics **48** Issue 1–3, (2008)179
- [5]. J.Rapp, et al., Journal of Nuclear Materials **337-339** (2005) 826
- [6]. G.Telesca, R. Zagorski et al., Journal of Nuclear Materials DOI: 10.1016/j.jnucmat.2013.01.118
- [7]. G.Telesca, R. Zagorski et al., Plasma Physics and Controlled Fusion **53** (2011) 115002.
- [8]. J. Mandrekas and W.M. Stacey, Nuclear Fusion **35** (1995) 843

- [9]. S.I. Braginskii, *Reviews of Plasma Physics* **1** (1965) 205
 [10]. Y.Yamamura, et al., Report of the IPP Nagoya, IPPJ-AM-26
 [11]. G. Telesca et al., *Contributions to Plasma Physics* **54** 1 – 6 (2014) / DOI 10.1002/ctpp.201410052
 [12]. N. Fedorczak et al., this Conference
 [13]. T. Pütterich et al., *2013 Plasma Physics and Controlled Fusion* **55** 124036
 [14]. R. Zagorski, et al., this Conference

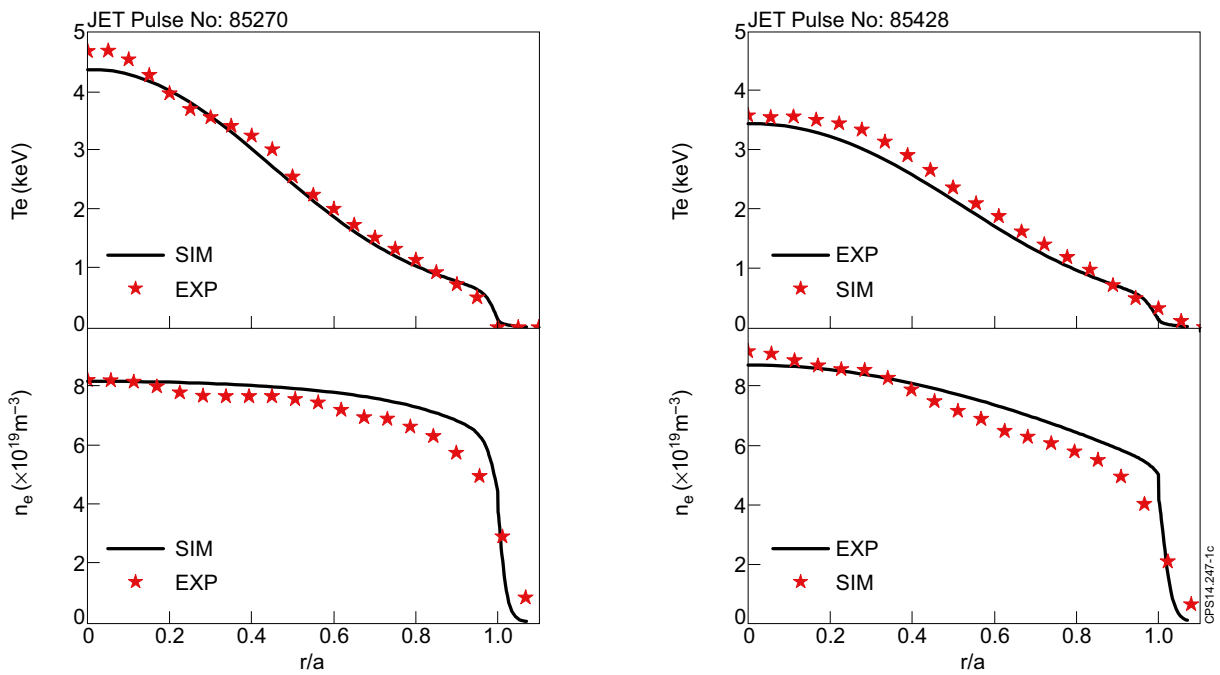


Figure 1. Top: T_e and n_e experimental and simulated profiles in the plasma core for the high-delta pulse. Bottom: T_e and n_e experimental and simulated profiles in the plasma core for the low-delta pulse.

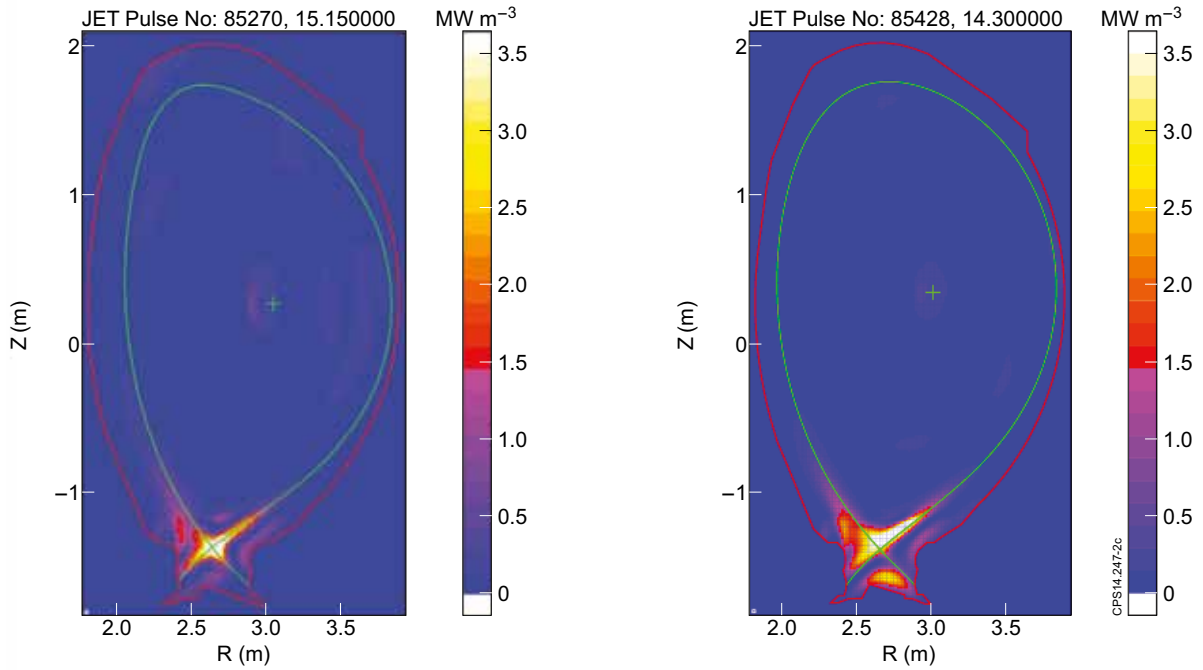


Figure 2. Tomographic 2D reconstruction of the radiated power density for high-delta (left) and low-delta (right) pulses. The high-delta pulse shows a significant radiation emitted in the plasma core, particularly at the low field side.

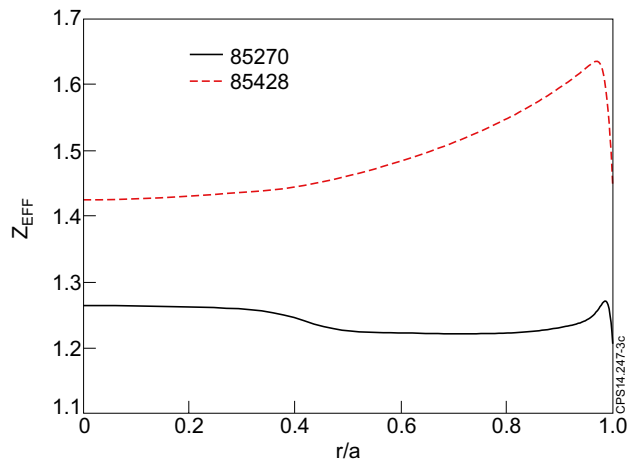


Figure 3. COREDIV Z_{eff} profiles for high-delta (black) and low-delta (red) pulses. Hollow Z_{eff} profile for low-delta is typical for Z_{eff} dominated by light impurities. The slight peaking in the centre for the high-delta, typical for Z_{eff} dominated by W, is due to higher central temperature (higher W ionization stages), not to W accumulation.